

# Airborne measurement of OH reactivity during INTEX-B

J. Mao<sup>1,\*</sup>, X. Ren<sup>1,\*\*</sup>, W. H. Brune<sup>1</sup>, J. R. Olson<sup>2</sup>, J. H. Crawford<sup>2</sup>, A. Fried<sup>3</sup>,  
L. G. Huey<sup>4</sup>, R. C. Cohen<sup>5</sup>, B. Heikes<sup>6</sup>, H. B. Singh<sup>7</sup>, D. R. Blake<sup>8</sup>, G. W. Sachse<sup>9</sup>,  
G. S. Diskin<sup>9</sup>, S. R. Hall<sup>10</sup>, and R. E. Shetter<sup>10</sup>

<sup>1</sup>Dept. of Meteorology, Pennsylvania State Univ., University Park, PA, USA

<sup>2</sup>Science Directorate, NASA Langley Research Center, Hampton, VA, USA

<sup>3</sup>Earth Observing Laboratory, National Center for Atmos. Research, Boulder, CO, USA

<sup>4</sup>School of Earth and Atmos. Sciences, Georgia Inst. of Technology, Atlanta, GA, USA

<sup>5</sup>Dept. of Chemistry and Dept. of Earth and Planet. Sci., Univ. of California Berkeley, CA, USA

<sup>6</sup>Graduate School of Oceanography, Univ. of Rhode Island, Narragansett, RI, USA

<sup>7</sup>NASA Ames Research Center, Moffett Field, CA, USA

<sup>8</sup>Dept. of Chemistry, Univ. of California, Irvine, CA, USA

<sup>9</sup>Science Directorate, NASA Langley Research Center, Hampton, VA, USA

<sup>10</sup>Atmos. Chemistry Division, National Center for Atmos. Research, Boulder, CO, USA

\* now at: School of Eng. and Applied Sciences, Harvard Univ., Cambridge, MA, USA

\*\* now at: Rosenstiel School of Marine and Atmos. Science, Univ. of Miami, Miami, FL, USA

Received: 1 July 2008 – Accepted: 1 July 2008 – Published: 24 July 2008

Correspondence to: J. Mao (mao@fas.harvard.edu)

Published by Copernicus Publications on behalf of the European Geosciences Union.

Airborne  
measurement of OH  
reactivity during  
INTEX-B

J. Mao et al.

Title Page

Abstract

Introduction

Conclusions

References

Tables

Figures

⏪

⏩

◀

▶

Back

Close

Full Screen / Esc

Printer-friendly Version

Interactive Discussion

## Abstract

The measurement of OH reactivity, the inverse of the OH lifetime, provides a powerful tool to investigate the atmospheric photochemistry. A new airborne OH reactivity instrument was designed and deployed for the first time on the NASA DC-8 aircraft during Intercontinental Chemical Transport Experiment-B (INTEX-B) campaign. The OH reactivity was measured by adding OH, generated by photolyzing water vapor with 185 nm UV light in a moveable wand, to the flow of ambient air in a flow tube and measuring the OH signal with laser induced fluorescence. As the wand was pulled back away from the OH detector, the OH signal decay was recorded; the slope of  $-\Delta \ln(\text{signal})/\Delta \text{time}$  was the OH reactivity. From the median vertical profile obtained in the second phase of INTEX-B, the measured OH reactivity ( $4.0 \pm 1.0 \text{ s}^{-1}$ ) is higher than the OH reactivity calculated from assuming that OH was in steady state ( $3.3 \pm 0.8 \text{ s}^{-1}$ ), and even higher than the OH reactivity that was calculated from the total measurements of all OH reactants ( $1.6 \pm 0.4 \text{ s}^{-1}$ ). Model calculations show that the missing OH reactivity is consistent with the over-predicted OH and under-predicted HCHO in the boundary layer and lower troposphere. The over-predicted OH and under-predicted HCHO suggest that the missing OH sinks are most likely related to some highly reactive VOCs that have HCHO as an oxidation product.

## 1 Introduction

The hydroxyl radical (OH) and the hydroperoxyl radical ( $\text{HO}_2$ ), collectively called  $\text{HO}_x$ , are central players in atmospheric chemistry. OH acts as the most important oxidizer and cleansing agent in the atmosphere on local to global scales. Its close chemical relative,  $\text{HO}_2$ , is a major precursor of tropospheric ozone.  $\text{HO}_x$  initiates and participates in almost all of the complex chemical pathways in the atmosphere. OH levels are largely determined by the atmospheric constituents emitted by biogenic and anthropogenic processes. To test the understanding of atmospheric OH, OH measurements

ACPD

8, 14217–14246, 2008

### Airborne measurement of OH reactivity during INTEX-B

J. Mao et al.

Title Page

Abstract

Introduction

Conclusions

References

Tables

Figures

◀

▶

◀

▶

Back

Close

Full Screen / Esc

Printer-friendly Version

Interactive Discussion

are typically compared to OH calculated by models that are constrained by simultaneous measurements of other atmospheric constituents. When measured and modeled OH disagree, the completeness of the measurement suite often comes into question.

The completeness of the measurement suite can be tested directly for atmospheric constituents that react with OH by measuring the OH reactivity, the inverse of the OH lifetime. The OH reactivity is the sum of the products of the concentrations and their reaction rate coefficients for all gases that react with OH. It is defined as:

$$k_{\text{OH}} = \sum k_{\text{OH}+\text{VOC}_i} [\text{VOC}_i] + k_{\text{OH}+\text{CO}} [\text{CO}] + k_{\text{OH}+\text{NO}} [\text{NO}] + k_{\text{OH}+\text{NO}_2} [\text{NO}_2] + k_{\text{OH}+\text{SO}_2} [\text{SO}_2] + \dots \quad (1)$$

Kovacs and Brune (2001) designed the first version OH reactivity instrument with flow tube technique, and successfully measured the ambient OH reactivity for the first time on the ground. This first version of OH reactivity instrument was also deployed in several other ground campaigns (Kovacs et al., 2003; Ren et al., 2003, 2004, 2006; Di Carlo et al., 2004; Shirley et al., 2006). The flash photolysis technique was developed by Jeanneret et al. (2001) and Sadanaga et al. (2004) for measuring the ambient OH reactivity. Sadanaga et al. (2005) successfully made field measurements in an urban area. These studies have demonstrated general agreement between measured and calculated OH reactivity for some urban environments and a surprising temperature dependent missing OH reactivity in forests (Di Carlo et al., 2004). More recently Sinha et al. (2008) developed a new method to measure OH reactivity by monitoring the change of OH reactants within the range of OH reactivity at  $6\sim 300\text{ s}^{-1}$ . Moreover, the OH reactivity measurements have proved valuable for examining OH sources using the assumption of the balance between OH production and loss. This paper presents a new airborne version of the Penn State OH reactivity instrument and the first airborne measurements of OH reactivity. The measurements were made during the NASA Intercontinental Chemical Transport Experiment-B (INTEX-B) mission in April/May 2006. The analysis includes comparisons of the measured OH reactivity with OH reactivity calculated by two independent methods as discussed later.

---

**Airborne  
measurement of OH  
reactivity during  
INTEX-B**J. Mao et al.

---

[Title Page](#)[Abstract](#)[Introduction](#)[Conclusions](#)[References](#)[Tables](#)[Figures](#)[⏪](#)[⏩](#)[◀](#)[▶](#)[Back](#)[Close](#)[Full Screen / Esc](#)[Printer-friendly Version](#)[Interactive Discussion](#)

## 2 Instrumentation

The OH reactivity,  $k_{\text{OH}}$  can be directly acquired by measuring OH decay rate as follows

$$\frac{d[\text{OH}]}{dt} = -k_{\text{OH}}[\text{OH}] \quad (2)$$

If the reactant concentrations change little when exposed to OH, the OH decay rate is assumed to be pseudo-first order (reactants remain constant). Assuming  $k_{\text{OH}}$  is constant during the decay, the OH reactivity can be determined from the equation:

$$k_{\text{OH}} = -\frac{\ln \frac{[\text{OH}]}{[\text{OH}]_0}}{\Delta t} \quad (3)$$

where  $[\text{OH}]_0$  represents the initial OH concentration, and  $[\text{OH}]$  represents the OH concentrations after a reaction time  $\Delta t$  between OH and its reactants.

The OH reactivity is measured by adding OH, which is generated by photolyzing water vapor with 185 nm ultraviolet light in a moveable wand, to the flow of ambient air and measuring the OH signal with laser induced fluorescence. The aluminum flow tube is 7.5 cm in diameter and 40 cm long between the inlet and the aluminum block that attaches to the OH detection system (Fig. 1a). The movable wand, which is 2.0 cm in diameter, is attached through a slot in the flow tube to a lead screw, which is turned by a stepper motor. As the wand is pulled back, the OH signal decay is recorded; the slope of  $-\frac{\ln \frac{[\text{OH}]}{[\text{OH}]_0}}{\Delta t}$  is the OH reactivity. Nine steps of 1.0 cm are used for each complete decay. The air flow velocity is approximately  $0.5 \text{ m s}^{-1}$ , so that each step is equivalent to  $\Delta t = 0.02 \text{ s}$ . The wand stays at each step for 20 s before moving in less than 0.5 s to the next step. Measuring the whole decay takes about 3.5 min. A sample decay obtained on the flight of 23 April 2006 shows the nine steps and the good linearity over three decay lifetimes (Fig. 1b). The linear regression algorithm is improved to remove the outliers in the decay, which could be due to the fast changing air mass the

### Airborne measurement of OH reactivity during INTEX-B

J. Mao et al.

Title Page

Abstract

Introduction

Conclusions

References

Tables

Figures

⏪

⏩

◀

▶

Back

Close

Full Screen / Esc

Printer-friendly Version

Interactive Discussion

aircraft encountered within each single decay of 3.5 min. The collected OH reactivity data shows very few decays were affected by the fast changing air mass during flight.

The OH signal is detected by Laser Induced Fluorescence (LIF) in a low pressure chamber (Faloona et al., 2004) OH is excited and emits fluorescence by the following process:



where  $X^2\Pi(v''=0)$  is the ground state of OH, and  $A^2\Sigma^+(v'=0)$  is the excited state. After absorbing laser light with a wavelength around 308 nm, the excited OH transits to the ground state spontaneously and emits fluorescence in the wavelength range from 307 nm to 311 nm simultaneously. The laser consists of a dye laser that is pumped by a diode-pumped Nd: YAG laser (Spectra-Physics, X30SC-1060A) at 3 kHz pulse frequency. The output of this dye laser is 308 nm UV light. Adjustment of laser wavelength can be achieved by an etalon.

The etalon is tuned on-line with OH fluorescence for 15 s and then off-line for 5 s to measure the background. The difference in the average on-line and average off-line signals is the OH fluorescence. The OH fluorescence is proportional to the OH mixing ratio. Because of this proportionality, the OH reactivity measurement does not require knowledge of the OH concentrations, although the OH detection system is calibrated.

The air sample is pulled into the vacuum detection system (from 3~12 hPa) through an orifice on a conic inlet (orifice ID is about 0.56 mm). This OH conic inlet sits 5 cm downstream of the flow tube. Inside the detection system, the laser beam crosses the detection axis that includes a gated microchannel plate (MCP) detector (Hamamatsu R2024U-06), which is set perpendicular to the airflow and the laser beam to detect the fluorescence emitted by the OH.

The OH reactivity instrument was installed in a rack in the forward cargo bay on the NASA DC-8. The inlet tube (1.5 cm dia.) protruded 10 cm below the aircraft skin. The end of the tube was cut at a 45° angle, facing forward, to create a ram force. This inlet was connected to the OH reactivity instrument with a 1 m long, 2.5 cm diameter

---

## Airborne measurement of OH reactivity during INTEX-B

J. Mao et al.

---

Title Page

Abstract

Introduction

Conclusions

References

Tables

Figures

⏪

⏩

◀

▶

Back

Close

Full Screen / Esc

Printer-friendly Version

Interactive Discussion

stainless steel flexible line. The air flowed through the instrument and down another line that was connected to an exhaust port downstream of the inlet.

The reaction time depends critically on the velocity of the air flow in the tube. The velocity is measured at the center of the flow tube just downstream of the OH detection system inlet with a hotwire anemometer (TSI 8455-03 Air Velocity Transducer). All the in situ velocity measurements from the hotwire anemometer need to be corrected by the ambient pressure and temperature to calculate the actual velocity inside the flow tube. This anemometer comes calibrated only for pressures near 1 atmospheric pressure, while the pressure inside the flow tube, which is equal to the ambient pressure, varied from 200 hPa~1000 hPa. Thus, the anemometer must be calibrated for low pressures.

To mimic the flow conditions during flight, the instrument was connected on the ground to a mass flow controller at the upstream end and to a vacuum pump at the downstream end. It was found that the reading of the transducer indicates the standard mass flow and shows no dependence on the pressure (from 20 kPa~100 kPa). Since the reading of the anemometer is a good indicator for the standard mass flow, tests were conducted to investigate the relationship between the anemometer reading and the actual mass flow. The reading of the anemometer at the farthest step of the wand has an excellent linear response to the mass flow.

The temperature increases by more than 30 K as the air speed relative to the aircraft decreases from the  $\sim 200 \text{ m s}^{-1}$  aircraft speed to less than a few m/s in the flow tube. This “stagnation” temperature increase can be calculated by Eq. (4).

$$V^2 = 2c_p(T - t) \quad (5)$$

where  $c_p$  is the specific heat capacity at constant pressure,  $V$  is the aircraft velocity,  $T$  is the stagnation temperature, and  $t$  is the static temperature. If the DC-8 aircraft flies at Mach 0.8, which is about  $270 \text{ m s}^{-1}$ ,  $c_p$  is about  $1000 \text{ J kg}^{-1} \text{ K}^{-1}$ , the air will be heated up by  $37^\circ\text{C}$  when it gets into the OH reactivity instrument flow tube. During the entire INTEX-B study, the lowest temperature inside the flow tube was 270 K when the

---

## Airborne measurement of OH reactivity during INTEX-B

J. Mao et al.

---

Title Page

Abstract

Introduction

Conclusions

References

Tables

Figures

⏪

⏩

◀

▶

Back

Close

Full Screen / Esc

Printer-friendly Version

Interactive Discussion

outside was about 220 K. To calculate the OH reactivity, both the ambient temperature and the temperature inside the flow tube are used, as will be discussed below.

During flight, the flow inside the tube was forced by a combination of ram pressure in the wedge-shaped inlet and the venturi effect on the outlet. An orifice inside the downstream line sets the velocity in the flow tube. The flow tube can be isolated from the atmosphere by two manual butterfly valves (Key High, ISO-KF Interface), which are upstream and downstream of the flow tube respectively.

The flow inside the flow tube was laminar, with the Reynolds number between 200 and 2000 depending on the altitude. However, the laminar parabolic profile was not fully developed. From entrance length theory, the characteristic length for the development of the parabolic velocity profile is given by  $l=0.065d \times Re$  under the laminar flow condition (Gerhart et al., 1992), where  $d$  is the diameter of the flow tube and  $Re$  is the Reynolds number. The entrance length in the OH reactivity instrument flow tube is estimated to be at least 100 cm, which is twice the length in the flow tube. Therefore, the flow velocity profile was fairly flat in the center and the velocity decreases near the walls. The instrument was frequently calibrated in flight to verify that the air flow in the flow tube is well understood. A mixture of 1% perfluoroethylene ( $C_3F_6$ ) in air was further diluted in zero air and added to the ambient air upstream of the flow tube. The  $C_3F_6$  reaction rate coefficient used for this calibration is  $(6.0 \pm 0.8) \times 10^{-13} \exp[(370 \pm 40)/T] \text{ cm}^3 \text{ molecule}^{-1} \text{ s}^{-1}$  (Dubey et al., 1996). Calibrations were performed at all altitudes, sometimes frequently (Fig. 2a). The median ratio of the measured-to-calculated OH reactivity for  $C_3F_6$  is  $1.12 \pm 0.36$  and is independent of altitude (Fig. 2b). The increased scatter in the ratio at lower altitudes probably comes from increased variability in the ambient OH reactivity, which must be subtracted from the OH reactivity measured during the calibration to get the measured OH reactivity due to  $C_3F_6$  alone. These calibrations verify that the flows in the OH reactivity instrument are well understood for the entire altitude range of the DC-8.

The OH reactivity instrument was also calibrated in the laboratory. Flight conditions were simulated by controlling the flow of zero air into the instrument with a mass flow

---

## Airborne measurement of OH reactivity during INTEX-B

J. Mao et al.

---

Title Page

Abstract

Introduction

Conclusions

References

Tables

Figures

⏪

⏩

◀

▶

Back

Close

Full Screen / Esc

Printer-friendly Version

Interactive Discussion

controller and by controlling the pressure in the flow tube with a vacuum pump downstream of the instrument. Four different calibration gases were added to the zero air upstream of the instrument at three different pressures. The measured OH reactivity was compared to the OH reactivity calculated from the well-known reaction rate coefficients and the known gas concentrations. These calibration gases were  $100 \pm 5$  ppmv carbon monoxide,  $10.3 \pm 0.5$  ppmv propane,  $0.92 \pm 0.05$  ppmv propene (MG Industries),  $1.029 \pm 0.009$  ppmv isoprene (Apel-Riemer Environmental, Inc.). The reaction rate coefficients are from Atkinson et al. (2006) and Sander et al. (2006). The comparison of the measured OH reactivity to the calculated reactivity is excellent for the three pressures (Fig. 3). This test indirectly validates the reaction rate coefficients for CO, isoprene, propane, and propene. Most importantly, it gives confidence in the OH reactivity instrument behavior at different pressures.

In regions where NO levels are greater than a few ppbv, the OH decay can be affected by the reaction of  $\text{HO}_2 + \text{NO} \rightarrow \text{OH} + \text{NO}_2$  inside the flow tube (Kovacs et al., 2003). The observed upward curvature in the decay curve can be corrected (Shirley et al., 2006). However, during the aircraft measurements of the second phase of INTEX-B, the sample air was relatively clean compared to the urban conditions. NO was typically much less than 1 ppbv and the  $\text{HO}_2 + \text{NO}$  reaction does not make much OH in the flow tube. Thus, the NO correction technique, which was used in the data analysis of ground-based studies, was not needed for these aircraft measurements.

The wall loss of OH increases the effective decay of measured OH and must be carefully characterized. It is inevitable that OH gets lost due to wall reactions. Wall loss could be reduced by using Teflon or another coating, but the wall loss could then change in unknown ways with the changes in the composition of the sampled ambient air. We prefer to have a steady and slightly larger wall loss that comes with an uncoated metal wall, for which OH is generally lost on each collision with the wall. Thus, the flow tube was not coated with any chemicals to reduce wall loss.

Wall loss reaction must be subtracted from the ambient measurement in order to obtain the measured OH reactivity. Wall loss can be estimated by finding the intercept

---

## Airborne measurement of OH reactivity during INTEX-B

J. Mao et al.

---

Title Page

Abstract

Introduction

Conclusions

References

Tables

Figures

⏪

⏩

◀

▶

Back

Close

Full Screen / Esc

Printer-friendly Version

Interactive Discussion



of linear regression of the measured OH reactivity versus the calculated OH reactivity or by measuring the OH decay in pure air or nitrogen carrier gases. The intercept method gives a median wall loss of  $2.9 \pm 0.3 \text{ s}^{-1}$ , while the pure carrier gas method gives an intercept of  $2.5 \pm 0.3 \text{ s}^{-1}$ . Both of these methods show that the wall loss is independent of pressure, as is expected by theory (Howard et al., 1979).

However, the wall loss measurement can be affected by trace impurities in the carrier gas for both methods. Thus a third way to find the wall loss is by measuring the OH reactivity in clean ambient air and subtracting the calculated OH reactivity due to measured atmospheric constituents from the measured OH reactivity. The lowest values at all altitudes will be the wall loss. The OH wall loss obtained from ambient measurements is  $2.0 \pm 0.3 \text{ s}^{-1}$ . This value is lower than that obtained from the other two methods, suggesting that the pure air and nitrogen do contain some impurities that react with OH. We use the value of  $2.0 \pm 0.3 \text{ s}^{-1}$  as the wall loss.

The uncertainty in the OH reactivity measurement consists of an absolute uncertainty and the uncertainty associated with the wall loss subtraction. The absolute uncertainty of OH reactivity measurement ( $2\sigma$ ) mainly depends on following factors:

1. uncertainty of the anemometer, which is 2% of reading from the manufacture specification for Model 8455-03 Air Velocity Transducer and 10% for the temperature and pressure correction;
2. uncertainty of the regression coefficients, which is 15% when the decay is less than  $2 \text{ s}^{-1}$ , and 5% when the decay is about  $6 \text{ s}^{-1}$ ;
3. the statistical precision of the fluorescence signals, which are about  $100 \text{ cts s}^{-1}$  for 15 s at the furthest point, for an uncertainty of 4%; and
4. uncertainty of the measured position of the wand, which is less than 1%.

Considering the uncertainty of the wall loss is  $0.3 \text{ s}^{-1}$  throughout the troposphere, the overall absolute uncertainty at the  $2\sigma$  confidence levels is about  $1 \text{ s}^{-1}$  at low altitudes

---

## Airborne measurement of OH reactivity during INTEX-B

J. Mao et al.

---

Title Page

Abstract

Introduction

Conclusions

References

Tables

Figures

⏪

⏩

◀

▶

Back

Close

Full Screen / Esc

Printer-friendly Version

Interactive Discussion

(for decay about  $6 \text{ s}^{-1}$ ), and  $0.7 \text{ s}^{-1}$  at high altitudes (for decay about  $2 \text{ s}^{-1}$ ). The uncertainty in the wall loss sets a minimum for the uncertainty in the measured OH reactivity when the OH reactivity is below  $1 \text{ s}^{-1}$ . Thus, the limit of detection for the OH reactivity measurement in INTEX-B was  $0.3 \text{ s}^{-1}$ , at the  $2\sigma$  confidence level.

### 3 Results

INTEX-B was a NASA project that aimed to understand the intercontinental transport and transformation of chemicals and aerosols and their impacts on air quality and climate (Singh et al., 2008)<sup>1</sup>. The platform of INTEX-B included four aircraft: the NASA DC-8, the NSF C-130, the NASA J-31 and the NASA B-200. The Penn State HO<sub>x</sub> and OH reactivity instruments were installed in the front cargo bay of the NASA DC-8 aircraft. The whole campaign lasted for 10 weeks (from 1 March 2006 to 15 May 2006) and was split into two phases. The first phase was focused on the Mexico City pollution outflow (from 1 March to 21 March, 9 flights) and was based in Houston, TX. The second phase was focused on the Asian pollution outflow (from 23 April to 15 May, 9 flights) and was based in Hawaii and Alaska.

These OH reactivity measurements were the first ever made from on an aircraft. During the first phase of INTEX-B, many adjustments had to be made to the instrument, particularly the air flow in the flow tube. After some tests and modifications, the instrument made measurements successfully in the second phase of the INTEX-B mission. The flight tracks of the second phase of INTEX-B were over the relatively clean Pacific Ocean with some flights over Alaska and the continental United States (Singh et al., 2008). The flight altitude was frequently changed, giving frequent scans over altitudes from 300 m to almost 12 km above the surface. These flight profiles allowed for a sig-

<sup>1</sup>Singh, H. B., Brune, W. H., Crawford, J. H., Jacob, D. J., Russell, P. B., et al.: An Overview of the INTEX-B Campaign: Transport and Transformation of Pollutants over the Pacific and the Gulf of Mexico, Atmos. Chem. Phys. Discuss., in preparation, 2008.

**Airborne  
measurement of OH  
reactivity during  
INTEX-B**

J. Mao et al.

Title Page

Abstract

Introduction

Conclusions

References

Tables

Figures

⏪

⏩

◀

▶

Back

Close

Full Screen / Esc

Printer-friendly Version

Interactive Discussion

nificant sampling of OH reactivity over the Pacific Ocean and near the western coast of North America.

### 3.1 Comparing measured and calculated OH reactivity

The measured OH reactivity is compared to OH reactivity that is calculated using two different methods. The first method is to determine the sum of the products of the measured concentrations of OH reactants and their reaction rate coefficients with OH. The second method is to assume that OH is in steady state; one then calculates the OH production, and finds the OH reactivity that balances the calculated OH production. In this paper, the OH reactivity calculated with the reactants is called “OHRreactants”; and the OH reactivity calculated from OH steady-state is called “OHRrecycling”.

The first method to calculate OH reactivity is to sum the products of all OH reactants concentrations and their reaction coefficients with OH, as in Eq. (1). This calculated OH reactivity should agree with the measured OH reactivity if all OH reactants have been measured. Comparing calculated and measured OH reactivity examines the current understanding of OH sinks in the atmosphere.

The measured OH reactants mainly include non-methane hydrocarbons (NMHC), oxygenated volatile organic compounds (OVOC), CO, CH<sub>4</sub>, HCHO, NO, NO<sub>2</sub>, SO<sub>2</sub>, HNO<sub>3</sub>, and H<sub>2</sub>O<sub>2</sub>. NMHC was measured by UC-Irvine and includes 26 alkanes, alkenes, alkynes, aromatics, nitrates, and halogenated compounds. OVOC was mainly measured by NASA Ames Research center and includes acetaldehyde, propanal, methanol, ethanol, acetone, and methyl ethyl ketone (MEK). The large OVOC component formaldehyde was measured by the NCAR tunable diode laser absorption spectrometer (TDLAS). CO was measured by NASA Langley Research Center also using a TDLAS. The reaction between OH and HNO<sub>4</sub> is not considered in this study because the HNO<sub>4</sub> measurements were made only in the middle and upper troposphere and its contribution to OH reactivity is relatively small. The reaction coefficients between OH and its reactants are acquired from JPL Chemical Kinetics and Photochemical Data Evaluation No. 15 (Sander et al., 2006) and Atkinson et al. (2006, 2007).

## Airborne measurement of OH reactivity during INTEX-B

J. Mao et al.

Title Page

Abstract

Introduction

Conclusions

References

Tables

Figures

⏪

⏩

◀

▶

Back

Close

Full Screen / Esc

Printer-friendly Version

Interactive Discussion



---

**Airborne  
measurement of OH  
reactivity during  
INTEX-B**J. Mao et al.

---

[Title Page](#)[Abstract](#)[Introduction](#)[Conclusions](#)[References](#)[Tables](#)[Figures](#)[⏪](#)[⏩](#)[◀](#)[▶](#)[Back](#)[Close](#)[Full Screen / Esc](#)[Printer-friendly Version](#)[Interactive Discussion](#)

The concentrations and reaction rate coefficients were affected by the pressure and temperature inside the flow tube. When the sampling air was introduced into the instrument during flight, the pressure inside the flow tube did not change but the temperature was elevated by about 40K when the aircraft was traveling at Mach 0.8. Thus, to compare the measured OH reactivity to the calculated OH reactivity, the calculated OH reactivity must use the concentrations and reaction rate coefficients at the flow tube temperature. If the measured and calculated OH reactivity agree, then the calculated OH reactivity can be corrected to ambient temperatures to determine the ambient OH reactivity.

For the air encountered in INTEX-B, the difference between the OH reactivity calculated at flow tube temperatures compared to the OH reactivity calculated at ambient temperatures was less than 15% for all data points. Calculations show that the difference is about  $0.12 \text{ s}^{-1}$  in the boundary layer and less than  $0.1 \text{ s}^{-1}$  in the upper troposphere. This difference is small because of the compensation by offsetting effects. The concentrations of the reactants decrease inside the flow tube by 10–15%. At the same time, the OH reaction rate coefficient for CO does not depend on temperature while those for  $\text{CH}_4$ ,  $\text{O}_3$ , and many NMHCs increase strongly with temperature, compensating for the decrease in reactant concentrations in the flow tube. Thus, the measured OH reactivity can be compared to the OH reactivity calculated for atmospheric temperatures with only a modest few percent increase in measurement uncertainty.

The median vertical profile (1 km each level) of the fractional contribution from main OH losses is calculated for ambient temperatures (Fig. 4). CO is a dominant OH loss throughout the troposphere, accounting for about 55% of total OH reactivity. In addition,  $\text{CH}_4$  contributes more to OH reactivity at low altitudes than at high altitudes, partly due to its temperature-dependent reaction coefficient with OH. The contribution from  $\text{O}_3$  is about 5% for all altitudes. OVOCs contribute about 15% to OH loss throughout the whole troposphere, which is significantly higher than the NMHCs' contribution. These contributions to the OH reactivity are probably typical of the air over relatively clean and relatively remote regions of the troposphere, far from local sources of pollution.

The second method to calculate OH reactivity is based on the assumption that OH is in steady state where the OH production rate equals the OH loss rate. Because the OH loss equals the OH reactivity multiplied by [OH], the sum of all known OH production rates divided by the OH concentration is equal to the OH reactivity:

$$5 \text{ OH Reactivity} = \frac{\text{Production of OH}}{[\text{OH}]} \quad (6)$$

This method is a good way to examine our current understanding of OH sources in the atmosphere. All known OH sources include  $\text{HO}_2 + \text{NO}$ ,  $\text{HO}_2 + \text{O}_3$ ,  $\text{O}^1\text{D} + \text{H}_2\text{O}$ , and the photolysis of  $\text{HNO}_3$ ,  $\text{CH}_3\text{COOH}$ , and  $\text{H}_2\text{O}_2$ . The photolysis reaction rate of  $\text{O}_3$ ,  $\text{HNO}_3$ ,  $\text{CH}_3\text{COOH}$ , and  $\text{H}_2\text{O}_2$  were measured by the NCAR spectrally resolved radiometer.

10 OH and  $\text{HO}_2$  were measured by the Penn State Airborne Tropospheric Hydrogen Oxides Sensor (ATHOS) based on Laser Induced Fluorescence.  $\text{O}_3$  was measured by NASA Langley fast response ozone measurements (FASTOZ) based on chemiluminescence. NO was measured by the Georgia Institute of Technology's NO measurement instrument using chemiluminescence.  $\text{H}_2\text{O}_2$  and  $\text{CH}_3\text{OOH}$  were measured by  
15 University of Rhode Island's HPLC-fluorometry instrument.  $\text{H}_2\text{O}$  was measured by NASA Langley's chilled mirror hygrometer.

To further investigate the contribution of OH sources, the fractional contribution from the different OH sources can be plotted as a function of altitude (Fig. 5). The median values are calculated based on all available measurements for each 1km layer from  
20 the surface to 12 km.

The  $\text{O}^1\text{D} + \text{H}_2\text{O}$  reaction is a dominant contributor in the lower troposphere, which contributes more than 50% of OH production in the marine boundary layer over the Pacific Ocean. Meanwhile the  $\text{HO}_2 + \text{NO}$  reaction dominates the OH production in the upper troposphere, where water vapor mixing ratios are relatively low and NO mixing  
25 ratios are relatively high. In addition, the  $\text{HO}_2 + \text{O}_3$  reaction also plays an important role for OH production throughout the whole altitude range.

The measured OH reactivity is compared to the OH reactivity that is calculated with the reactants using the later method (OHRreactants) and the OH reactivity that is cal-

---

**Airborne  
measurement of OH  
reactivity during  
INTEX-B**J. Mao et al.

---

Title Page

Abstract

Introduction

Conclusions

References

Tables

Figures

⏪

⏩

◀

▶

Back

Close

Full Screen / Esc

Printer-friendly Version

Interactive Discussion



culated from OH steady-state is (OHRrecycling) in Fig. 6. There are periods when the measured and calculated OH reactivity values all agree to within uncertainties, especially at lower values of OH reactivity. However, when the measured OH reactivity exceeds a few  $s^{-1}$ , the measured OH reactivity is typically greater than OHRcycling, which is typically greater than OHRreactants. These differences can be quite large (e.g., at day-of-the-year time 135.93 in Fig. 6).

To study the dependence of the measurement with altitude, the median vertical profile (1 km each level) of the measured OH reactivity is plotted against the altitude in Fig. 7. The median values are calculated based on all measured OH reactivity in each 1-km layer through the whole troposphere. Medians, interquartile range (25%–75%), and 1.5 times interquartile range (12.5%–87.5%) are all presented for each level.

The measured OH reactivity, OHRcycling, and OHRreactants have similar trends from low altitude to high altitude – they decrease to values less than  $1 s^{-1}$  at the highest altitudes. However, in the 0–2-km layer, the median measured OH reactivity ( $4.0 \pm 1.0 s^{-1}$ ) is greater than the median OHRcycling ( $3.3 \pm 0.8 s^{-1}$ ), and even greater than the median OHRreactants ( $1.6 \pm 0.4 s^{-1}$ ). The uncertainty of OHRcycling is calculated based on the uncertainties of measured  $HO_2/OH$  ratio and the OH concentration. The uncertainty of OHRreactants is based on the uncertainties of all measured OH reactants and their reaction coefficients with OH. The differences between OHRreactants and the other two methods are statistically significant because the OHRreactants falls out of the observation uncertainties range in the lowest layer. If the wall loss is  $2.5\text{--}2.9 s^{-1}$  as suggested by laboratory tests, then the measured OH reactivity and OHRcycling would agree, although the difference between with the measured OH reactivity and OHRreactant would still be significant. The measured OH reactivity is also greater than both OHRcycling and OHRreactants above 2 km.

To verify this conclusion, a two-sample *t*-test is conducted between the OHRreactant and OHRcycling and the results show that these two variables are significantly different with the confidence interval 99%. The significance is also proved between the measured OH reactivity and OHRreactant. The difference between the measured OH

---

**Airborne  
measurement of OH  
reactivity during  
INTEX-B**J. Mao et al.

---

[Title Page](#)[Abstract](#)[Introduction](#)[Conclusions](#)[References](#)[Tables](#)[Figures](#)[⏪](#)[⏩](#)[◀](#)[▶](#)[Back](#)[Close](#)[Full Screen / Esc](#)[Printer-friendly Version](#)[Interactive Discussion](#)

reactivity and OHRreactants suggests the presence of unknown OH reactants in the boundary layer that can affect the OH reactivity up to 4 km or so. This difference also suggests that about half of the OH reactivity is missing at these lower altitudes. Although the difference between the measured OH reactivity and OHRreactants extends higher than 2 km, it becomes less and statistically insignificant.

Some unmeasured oxidation products of hydrocarbons and other atmospheric constituents can react with OH. These were not in the list of atmospheric constituents used to calculate OHRreactants. However, when the additional OH reactivity that is calculated from the intermediates that are modeled but not measured, OHRreactants increases by at most  $0.1 \text{ s}^{-1}$ , less than 5% of OHRreactants. These intermediate reaction products cannot account for the missing OH reactivity.

The differences between the measured OH reactivity and OHRreactants should be reflected in the differences between measured and modeled OH, because the modeled OH uses the same OH reactants and reaction rate coefficients as OHRreactants. A chemical box model is used by NASA Langley Research Center to calculate the OH and HO<sub>2</sub> (called “LaRC model” in this paper). The model detail is described elsewhere (Crawford et al., 1999; Olson et al., 2004). The model is constrained by the observations of O<sub>3</sub>, CO, NO<sub>2</sub>, NO, NMHC, acetone, methanol, dew point, temperature, pressure, and photolysis frequencies. Diurnal steady-state means that the model is run repeatedly over an entire day using the observed conditions until the concentrations of longer lived species like H<sub>2</sub>O<sub>2</sub> do not change for any given time of day. The advantage of this method is to ensure the long-lived species are eventually in balance with other species.

Figure 8 presents the vertical profile of measured and modeled OH, HO<sub>2</sub> and HCHO during the second phase of INTEX-B. The measured and modeled OH and HO<sub>2</sub> disagree the most below 2 km altitude and then gradually come into agreement above 4 km altitude (Figure 8). Below 2 km, the model calculation of OH is about 30% higher than the measurement. Meanwhile, the model calculation of HO<sub>2</sub> agrees very well with the measurement. Since OH and HO<sub>2</sub> were measured simultaneously in ATHOS

---

## Airborne measurement of OH reactivity during INTEX-B

J. Mao et al.

---

Title Page

Abstract

Introduction

Conclusions

References

Tables

Figures

⏪

⏩

◀

▶

Back

Close

Full Screen / Esc

Printer-friendly Version

Interactive Discussion



instrument (Faloona et al., 2004), this difference is unlikely from absolute instrument artifacts only. If OH reactivity were missing from the model below 2 km, as Fig. 8 suggests, then there would be less OH loss in the model because the model uses only the measured atmospheric species. These are the same reactants with OH that go into the OHRreactants. This observation of missing OH reactivity is consistent with the over-predicted OH.

As an intermediate product from VOC oxidation, formaldehyde (HCHO) is a good indicator for hydrocarbon photochemistry because it is a product of oxidation of hydrocarbons by OH. Moreover, HCHO is not constrained in the LaRC model simulation. It is worthwhile to compare the modeled and measured HCHO. This comparison will examine our understanding of the photochemistry from another independent instrument. As shown in Fig. 8, the most under-predicted HCHO appears at altitudes from the surface to 2 km height. Could this extra amount of HCHO be from some atmospheric constituents that contribute to the missing OH reactivity? Could this missing OH reactivity come from highly reactive VOCs, or some other sulfuric, halogenated species? From the analysis of individual flights, we have noticed that the difference between measurement and OHRreactants appears when HCHO reaches a peak. As shown in Fig. 9, the difference between the OH reactivity measurement and OHRreactants is correlated with HCHO concentration below 2 km when NO is below 100 pptv, with a correlation coefficient  $R^2=0.58$ . This correlation indicates indirectly that the missing OH reactivity could be from some highly reactive VOCs that have HCHO as a product of oxidation.

From all the analysis above, the over-predicted OH and under-predicted HCHO are consistent with the missing OH reactivity, which is the measured OH reactivity – OHRreactants. Since 1000 pptv HCHO contributes less than  $0.2 \text{ s}^{-1}$  OH reactivity in the boundary layer, it is more likely that HCHO serves as an indicator instead of contributing a big part to the missing OH reactivity. On the other hand, if we assume the missing OH reactivity is from some other oxygenated VOCs and we increase the current acetaldehyde concentration by a factor of 10 in the boundary layer, model calcu-

---

## Airborne measurement of OH reactivity during INTEX-B

J. Mao et al.

---

Title Page

Abstract

Introduction

Conclusions

References

Tables

Figures

⏪

⏩

◀

▶

Back

Close

Full Screen / Esc

Printer-friendly Version

Interactive Discussion



lations show that the total OH reactivity increases by 40%, OH decreases 65%, HCHO increases 65% and HO<sub>2</sub> decreases 15%. HO<sub>2</sub> is less sensitive than OH and HCHO in the model responding to the extra acetaldehyde. Qualitatively these model outputs agree well with the over-predicted OH and under-predicted HCHO for the missing OH reactivity. This will shed some light on finding the missing species and thus reconciling the model and measurements.

## 4 Summary

A new airborne version of OH reactivity instrument was developed and tested on the NASA DC-8 aircraft. OH reactivity was successfully measured for the first time above Earth's surface during the second phase of the INTEX-B aircraft mission. The *in situ* and laboratory calibrations indicate good response of this new instrument under different pressure conditions. For INTEX-B Phase II, which was conducted mainly over Pacific Ocean, the OH reactivity measurements are reasonable compared to two kinds of calculated OH reactivity, calculated with the measured OH reactants and calculated from OH steady-state. They all show the trend of OH reactivity decreasing with altitude. However, a difference between the measurements and calculations exists at altitudes below 4 km and is most pronounced in the 0~2 km layer. The measured OH reactivity ( $4.0 \pm 1.0 \text{ s}^{-1}$ ) is larger than the calculated OH reactivity from cycling ( $3.3 \pm 0.8 \text{ s}^{-1}$ ), and even larger than the calculated OH reactivity from the total measurements of all OH reactants ( $1.6 \pm 0.4 \text{ s}^{-1}$ ). Model calculation shows the missing OH reactivity is qualitatively consistent with the over-predicted OH and under-predicted HCHO in the 0~2 km layer. The missing OH reactivity is correlated with HCHO in this layer, suggesting that it is most likely related to some highly reactive VOCs that are missing in the measurements and have HCHO as a product of oxidation. The missing OH reactivity in the boundary layer indicates the shorter OH lifetime, and thus implies the longer lifetimes for CH<sub>4</sub>, CO and NO<sub>2</sub> than in current models.

### Airborne measurement of OH reactivity during INTEX-B

J. Mao et al.

Title Page

Abstract

Introduction

Conclusions

References

Tables

Figures

⏪

⏩

◀

▶

Back

Close

Full Screen / Esc

Printer-friendly Version

Interactive Discussion

*Acknowledgements.* This research was supported by the NASA Tropospheric Chemistry Program through NASA grant NNG06GA94G. We also would like to thank machine shop staff of the College of Earth and Mineral Sciences for their major contributions to the development and fabrication of this instrument. We thank the NASA DC-8 crew for their generous help for putting the instrument on the aircraft. J. Mao also thanks R. E. Shetter for the frequent opportunities to fly on the DC-8 to test and improve the instrument performance.

## References

- Atkinson, R., Baulch, D. L., Cox, R. A., Crowley, J. N., Hampson, R. F., Hynes, R. G., Jenkin, M. E., Rossi, M. J., Troe, J., and IUPAC Subcommittee: Evaluated kinetic and photochemical data for atmospheric chemistry: Volume II: gas phase reactions of organic species, *Atmos. Chem. Phys.*, 6, 3625–4055, 2006, <http://www.atmos-chem-phys.net/6/3625/2006/>.
- Atkinson, R., Baulch, D. L., Cox, R. A., Crowley, J. N., Hampson, R. F., Hynes, R. G., Jenkin, M. E., Rossi, M. J., and Troe, J.: Evaluated kinetic and photochemical data for atmospheric chemistry: Volume III: gas phase reactions of inorganic halogens, *Atmos. Chem. Phys.*, 7, 981–1191, 2007, <http://www.atmos-chem-phys.net/7/981/2007/>.
- Crawford, J., Davis, D., Olson, J., Chen, G., Liu, S., Gregory, G., Barrick, J., Sachse, G., Sandholm, S., Heikes, B., Singh, H., and Blake, D.: Assessment of upper tropospheric HO<sub>x</sub> sources over the tropical Pacific based on NASA GTE/PEM data: Net effect on HO<sub>x</sub> and other photochemical parameters, *J. Geophys. Res.-Atmos.*, 104, 16255–16273, 1999.
- Di Carlo, P., Brune, W. H., Martinez, M., Harder, H., Leshner, R., Ren, X. R., Thornberry, T., Carroll, M. A., Young, V., Shepson, P. B., Riemer, D., Apel, E., and Campbell, C.: Missing OH reactivity in a forest: Evidence for unknown reactive biogenic VOCs, *Science*, 304, 722–725, 2004.
- Dubey, M. K., Hanisco, T. F., Wennberg, P. O., and Anderson, J. G.: Monitoring potential photochemical interference in laser-induced fluorescence measurements of atmospheric OH, *Geophys. Res. Lett.*, 23, 3215–3218, 1996.
- Faloon, I. C., Tan, D., Leshner, R. L., Hazen, N. L., Frame, C. L., Simpas, J. B., Harder, H., Martinez, M., Di Carlo, P., Ren, X. R., and Brune, W. H.: A laser-induced fluorescence

**Airborne  
measurement of OH  
reactivity during  
INTEX-B**

J. Mao et al.

Title Page

Abstract

Introduction

Conclusions

References

Tables

Figures

⏪

⏩

◀

▶

Back

Close

Full Screen / Esc

Printer-friendly Version

Interactive Discussion

- instrument for detecting tropospheric OH and HO<sub>2</sub>: characteristics and calibration, *J. Atmos. Chem.*, 47, 139–167, 2004.
- Jeanneret, F., Kirchner, F., Clappier, A., van den Bergh, H., and Calpini, B.: Total VOC reactivity in the planetary boundary layer – 1: Estimation by a pump and probe OH experiment, *J. Geophys. Res.-Atmos.*, 106, 3083–3093, 2001.
- Kovacs, T. A. and Brune, W. H.: Total OH loss rate measurement, *J. Atmos. Chem.*, 39, 105–122, 2001.
- Kovacs, T. A., Brune, W. H., Harder, H., Martinez, M., Simpas, J. B., Frost, G. J., Williams, E., Jobson, T., Stroud, C., Young, V., Fried, A., and Wert, B.: Direct measurements of urban OH reactivity during Nashville SOS in summer 1999, *J. Environ. Monitor.*, 5, 68–74, 2003.
- Olson, J. R., Crawford, J. H., Chen, G., Fried, A., Evans, M. J., Jordan, C. E., Sandholm, S. T., Davis, D. D., Anderson, B. E., Avery, M. A., Barrick, J. D., Blake, D. R., Brune, W. H., Eisele, F. L., Flocke, F., Harder, H., Jacob, D. J., Kondo, Y., Lefer, B. L., Martinez, M., Mauldin, R. L., Sachse, G. W., Shetter, R. E., Singh, H. B., Talbot, R. W., and Tan, D.: Testing fast photochemical theory during TRACE-P based on measurements of OH, HO<sub>2</sub>, and CH<sub>2</sub>O, *J. Geophys. Res.-Atmos.*, 109(16), D15S10, doi:10.1029/2003JD004278, 2004.
- Ren, X. R., Harder, H., Martinez, M., Leshner, R. L., Oligier, A., Shirley, T., Adams, J., Simpas, J. B., and Brune, W. H.: HO<sub>x</sub> concentrations and OH reactivity observations in New York City during PMTACS-NY2001, *Atmos. Environ.*, 37, 3627–3637, 2003.
- Ren, X. R., Harder, H., Martinez, M., Faloon, I. C., Tan, D., Leshner, R. L., Di Carlo, P., Simpas, J. B., and Brune, W. H.: Interference testing for atmospheric HO<sub>x</sub> measurements by laser-induced fluorescence, *J. Atmos. Chem.*, 47, 169–190, 2004.
- Ren, X. R., Brune, W. H., Oligier, A., Metcalf, A. R., Simpas, J. B., Shirley, T., Schwab, J. J., Bai, C. H., Roychowdhury, U., Li, Y. Q., Cai, C. X., Demerjian, K. L., He, Y., Zhou, X. L., Gao, H. L., and Hou, J.: OH, HO<sub>2</sub>, and OH reactivity during the PMTACS-NY Whiteface Mountain 2002 campaign: Observations and model comparison, *J. Geophys. Res.-Atmos.*, 111(12), D10S03, doi:10.1029/2005JD006126, 2006.
- Sadanaga, Y., Yoshino, A., Watanabe, K., Yoshioka, A., Wakazono, Y., Kanaya, Y., and Kajii, Y.: Development of a measurement system of OH reactivity in the atmosphere by using a laser-induced pump and probe technique, *Rev. Sci. Instrum.*, 75, 2648–2655, 2004.
- Sadanaga, Y., Yoshino, A., Kato, S., and Kajii, Y.: Measurements of OH reactivity and photochemical ozone production in the urban atmosphere, *Environ. Sci. Technol.*, 39, 8847–8852, 2005.

---

**Airborne  
measurement of OH  
reactivity during  
INTEX-B**J. Mao et al.

---

[Title Page](#)[Abstract](#)[Introduction](#)[Conclusions](#)[References](#)[Tables](#)[Figures](#)[⏪](#)[⏩](#)[◀](#)[▶](#)[Back](#)[Close](#)[Full Screen / Esc](#)[Printer-friendly Version](#)[Interactive Discussion](#)

- Sander, S. P., Friedl, R. R., Ravishankara, A. R., Golden, D. M., Kurylo, M. J., Molina, M. J., Moortgat, G. K., Keller-Rudek, H., Finlayson-Pitts, B. J., Wine, P. H., Huie, R. E., and Orkin, V. L.: Chemical Kinetics and Photochemical Data for Use in Atmospheric Studies Evaluation Number 15, JPL Publication 06-2, Jet Propulsion Laboratory, Pasadena, CA, USA, 2006.
- 5 Shirley, T. R., Brune, W. H., Ren, X., Mao, J., Leshner, R., Cardenas, B., Volkamer, R., Molina, L. T., Molina, M. J., Lamb, B., Velasco, E., Jobson, T., and Alexander, M.: Atmospheric oxidation in the Mexico City Metropolitan Area (MCMA) during April 2003, *Atmos. Chem. Phys.*, 6, 2753–2765, 2006,  
<http://www.atmos-chem-phys.net/6/2753/2006/>.
- 10 Sinha, V., Williams, J., Crowley, J. N., and Lelieveld, J.: The comparative reactivity method: a new tool to measure total OH reactivity in ambient air, *Atmos. Chem. Phys.*, 8, 2213–2227, 2008,  
<http://www.atmos-chem-phys.net/8/2213/2008/>.

ACPD

8, 14217–14246, 2008

**Airborne  
measurement of OH  
reactivity during  
INTEX-B**

J. Mao et al.

Title Page

Abstract

Introduction

Conclusions

References

Tables

Figures

⏪

⏩

◀

▶

Back

Close

Full Screen / Esc

Printer-friendly Version

Interactive Discussion

**Table 1.** Measurements on NASA DC-8 airplane during INTEX-B.

Chemicals	Methods	Organization
photolysis frequencies	actinic flux spectroradiometer	NCAR
OH, HO <sub>2</sub>	laser induced fluorescence	Penn State University
H <sub>2</sub> O	chilled mirror hygrometer	NASA Langley Research Center
NO	chemiluminescence	Georgia Tech
NO <sub>2</sub>	laser induced fluorescence	UC-Berkley
O <sub>3</sub>	chemiluminescence	NASA Langley Research Center
H <sub>2</sub> O <sub>2</sub> CH <sub>3</sub> COOH	HPLC-fluorometry	University of Rhode Island
CO, CH <sub>4</sub>	tunable diode laser absorption spectrometry	NASA Langley Research Center
HCHO	tunable diode laser absorption spectrometry	NCAR
SO <sub>2</sub>	chemical ionization mass spectrometry	Georgia Tech
HNO <sub>3</sub>	mist chamber/GC-IC	University of New Hampshire
NMHC <sup>a</sup>	whole air sample collection, GC-FID/EC/MS analysis	UC-Irvine
OVOC <sup>b</sup> , Nitriles, PANs	GC-ECD/PID/RGD	NASA Ames Research Center

<sup>a</sup> NMHC includes ethane, ethene, propane, propene, i-butane, n-butane, ethyne, i-pentane, n-pentane, n-hexane, isoprene, benzene, and toluene.

<sup>b</sup> OVOC includes acetaldehyde, propanal, acetone, MEK, methanol, and ethanol.

**Airborne  
measurement of OH  
reactivity during  
INTEX-B**

J. Mao et al.

Title Page

Abstract

Introduction

Conclusions

References

Tables

Figures

◀

▶

◀

▶

Back

Close

Full Screen / Esc

Printer-friendly Version

Interactive Discussion



## Airborne measurement of OH reactivity during INTEX-B

J. Mao et al.

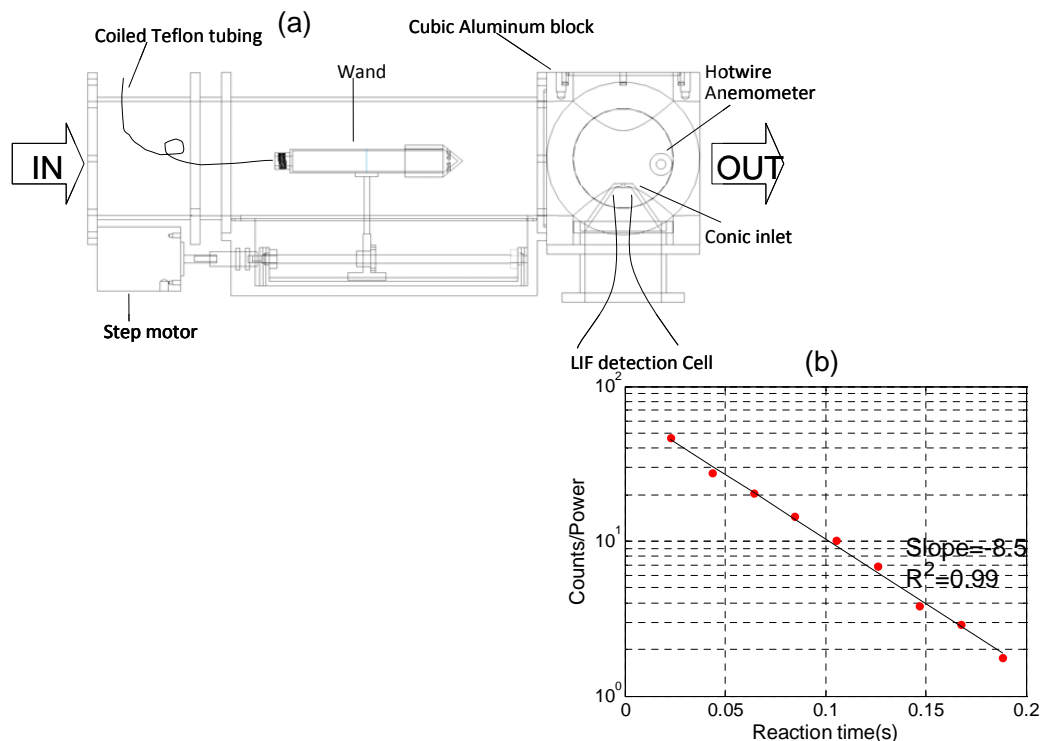


**Fig. 1.** Schematic diagram (a) and sample decay (b) of the OH reactivity instrument. In the schematic diagram (a), the left part is the aluminum flow tube with the linear transmission system sitting below the tube. The right part is the cubic aluminum block with conic inlet for OH detection. The sample air flows in from the left side of the flow tube, reacts with the OH injected out from the wand, and flow out from the right side of the cubic aluminum block. The sample decay (b) was obtained on the 23 April 2006 flight when flying through the boundary layer. In this case, the measured OH reactivity is about  $6.5 \text{ s}^{-1}$  ( $8.5 \text{ s}^{-1}$  minus wall loss of  $2.0 \text{ s}^{-1}$ ).

Title Page

Abstract

Introduction

Conclusions

References

Tables

Figures

◀

▶

◀

▶

Back

Close

Full Screen / Esc

Printer-friendly Version

Interactive Discussion

Airborne  
measurement of OH  
reactivity during  
INTEX-B

J. Mao et al.

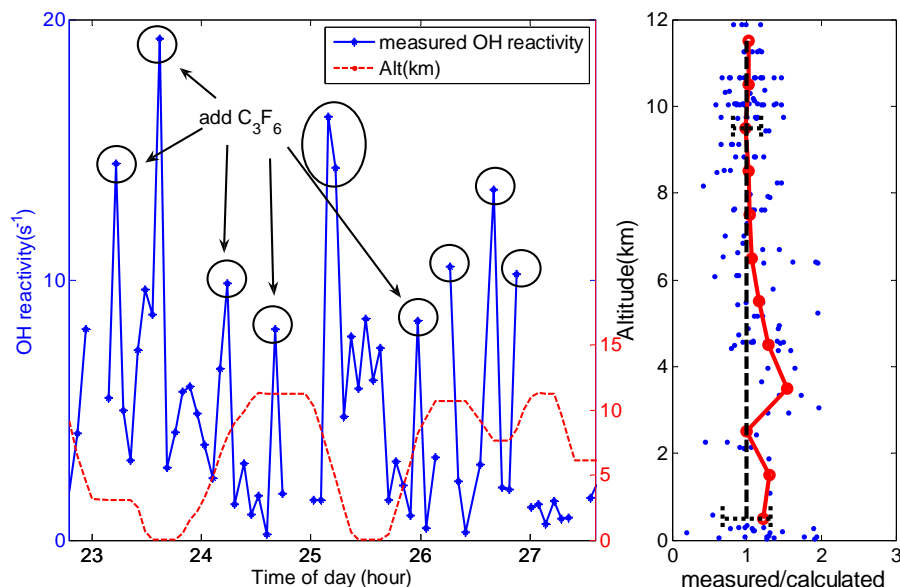


**Fig. 2.** In situ  $C_3F_6$  calibration on the flight of 23 April 2006 during the INTEX-B field campaign. **(a)** Measured OH reactivity without  $C_3F_6$  added (points and lines), with  $C_3F_6$  added (circled points), and altitude (dashed line). **(b)** The ratio of the measured-to-calculated OH reactivity due to  $C_3F_6$  calibrations (points) and the median ratio for each kilometer of altitude (line with points). The dashed line is the one-to-one line and the dotted lines are the  $2\sigma$  uncertainties.

[Title Page](#)[Abstract](#)[Introduction](#)[Conclusions](#)[References](#)[Tables](#)[Figures](#)[◀](#)[▶](#)[◀](#)[▶](#)[Back](#)[Close](#)[Full Screen / Esc](#)[Printer-friendly Version](#)[Interactive Discussion](#)

Airborne  
measurement of OH  
reactivity during  
INTEX-B

J. Mao et al.

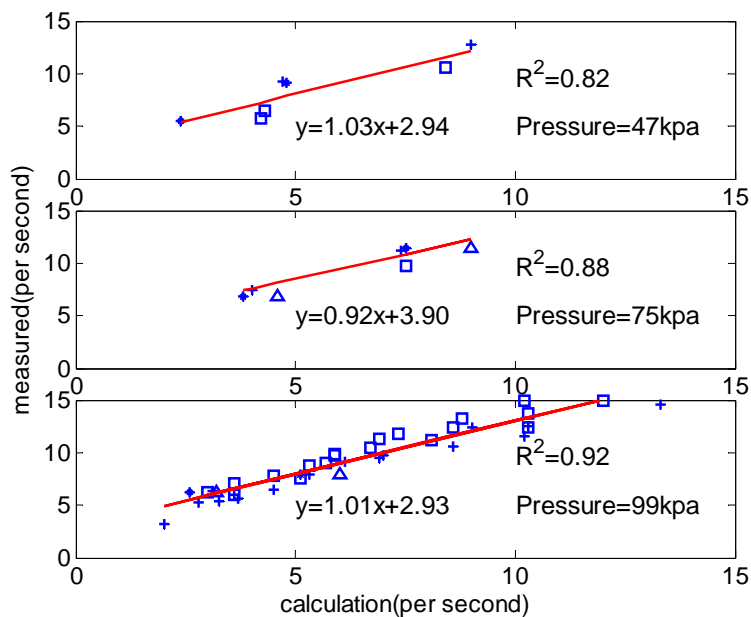


**Fig. 3.** Laboratory calibration for the OH reactivity instrument using different gases at different pressures. The measured OH reactivity is plotted versus the calculated OH reactivity. Calibration gases include CO (hollow square), isoprene (plus sign), propane (star) and propene (triangle).

[Title Page](#)[Abstract](#)[Introduction](#)[Conclusions](#)[References](#)[Tables](#)[Figures](#)[◀](#)[▶](#)[◀](#)[▶](#)[Back](#)[Close](#)[Full Screen / Esc](#)[Printer-friendly Version](#)[Interactive Discussion](#)



Airborne  
measurement of OH  
reactivity during  
INTEX-B

J. Mao et al.

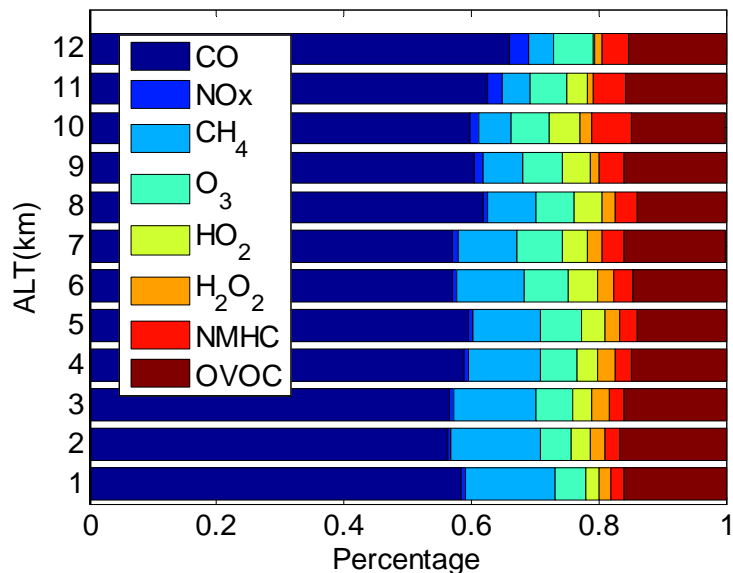


**Fig. 4.** The median vertical profile of fractional contribution from the main OH losses through the troposphere during the second phase of INTEX-B field campaign. The OH losses include the reactions between OH and its reactants, including CO, NO<sub>x</sub>, CH<sub>4</sub>, O<sub>3</sub>, HO<sub>2</sub>, H<sub>2</sub>O<sub>2</sub>, NMHC, and OVOC.

[Title Page](#)[Abstract](#)[Introduction](#)[Conclusions](#)[References](#)[Tables](#)[Figures](#)[◀](#)[▶](#)[◀](#)[▶](#)[Back](#)[Close](#)[Full Screen / Esc](#)[Printer-friendly Version](#)[Interactive Discussion](#)

Airborne  
measurement of OH  
reactivity during  
INTEX-B

J. Mao et al.

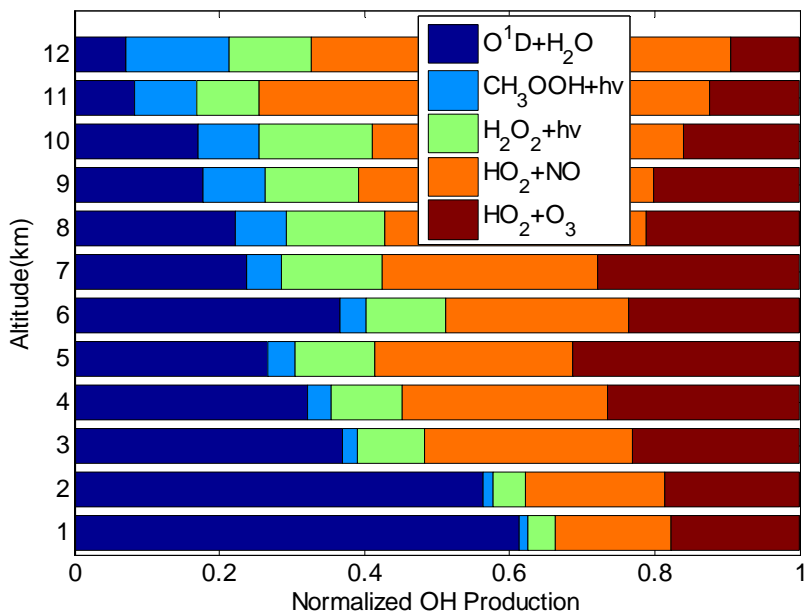


**Fig. 5.** Fractional contribution of different kinds of OH sources through troposphere in INTEX-B field campaign. OH sources include O(<sup>1</sup>D)+H<sub>2</sub>O, HO<sub>2</sub>+NO, HO<sub>2</sub>+O<sub>3</sub>, the photolysis of CH<sub>3</sub>OOH, H<sub>2</sub>O<sub>2</sub> and HNO<sub>3</sub>.

[Title Page](#)[Abstract](#)[Introduction](#)[Conclusions](#)[References](#)[Tables](#)[Figures](#)[⏪](#)[⏩](#)[◀](#)[▶](#)[Back](#)[Close](#)[Full Screen / Esc](#)[Printer-friendly Version](#)[Interactive Discussion](#)

Airborne  
measurement of OH  
reactivity during  
INTEX-B

J. Mao et al.

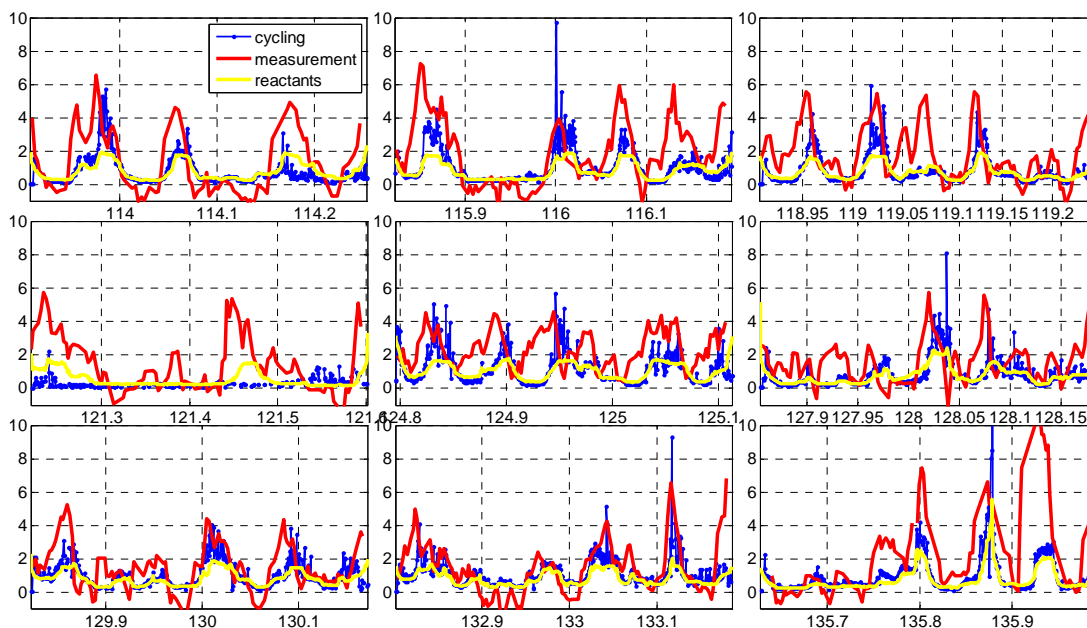


**Fig. 6.** OH reactivity measurement during the second phase of INTEX-B. Each panel is for one single flight. In each panel, the X-axis is Julian day and the Y-axis is the three types of OH reactivity discussed in the text, the measured OH reactivity (red), the calculated OH reactivity based on cycling (blue) and the calculated OH reactivity based on all measured reactants (yellow). The measured OH reactivity has been smoothed with a 3-point running average.

[Title Page](#)[Abstract](#)[Introduction](#)[Conclusions](#)[References](#)[Tables](#)[Figures](#)[⏪](#)[⏩](#)[◀](#)[▶](#)[Back](#)[Close](#)[Full Screen / Esc](#)[Printer-friendly Version](#)[Interactive Discussion](#)

Airborne  
measurement of OH  
reactivity during  
INTEX-B

J. Mao et al.

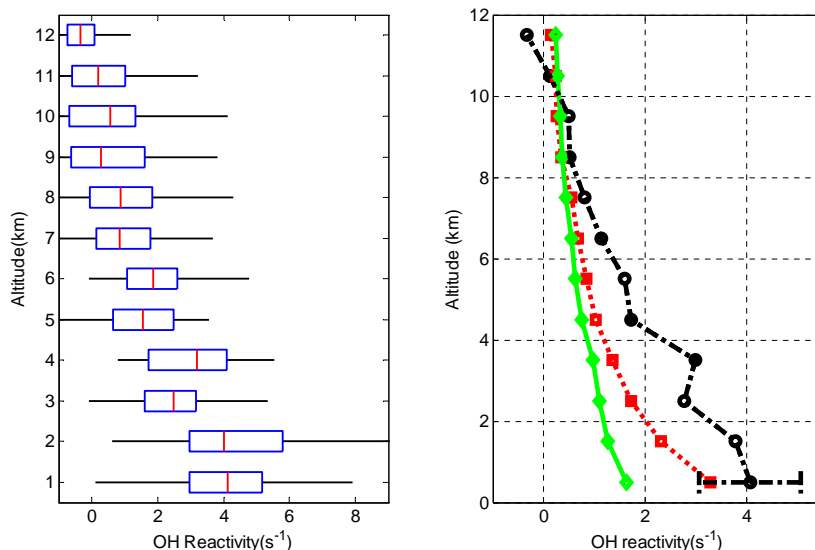


**Fig. 7.** Measured OH reactivity (left) and the comparison (right) of the three types of OH reactivity through the troposphere during the second phase of INTEX-B field campaign. In the left panel, the two ends of the box show the lower quartile, and upper quartile values. The line inside the box shows the median value. The lines extending from each end of the box shows the extent of the rest of the data (1.5 times the interquartile range). In the right panel, the dash-dotted line with circles is the median measured OH reactivity, the dotted line with squares is the median OHRrecycling, and the solid line with diamonds is the median OHRreactants. The horizontal bar indicates the uncertainties ( $2\sigma$ ) of the observations.

[Title Page](#)[Abstract](#)[Introduction](#)[Conclusions](#)[References](#)[Tables](#)[Figures](#)[◀](#)[▶](#)[◀](#)[▶](#)[Back](#)[Close](#)[Full Screen / Esc](#)[Printer-friendly Version](#)[Interactive Discussion](#)

Airborne  
measurement of OH  
reactivity during  
INTEX-B

J. Mao et al.

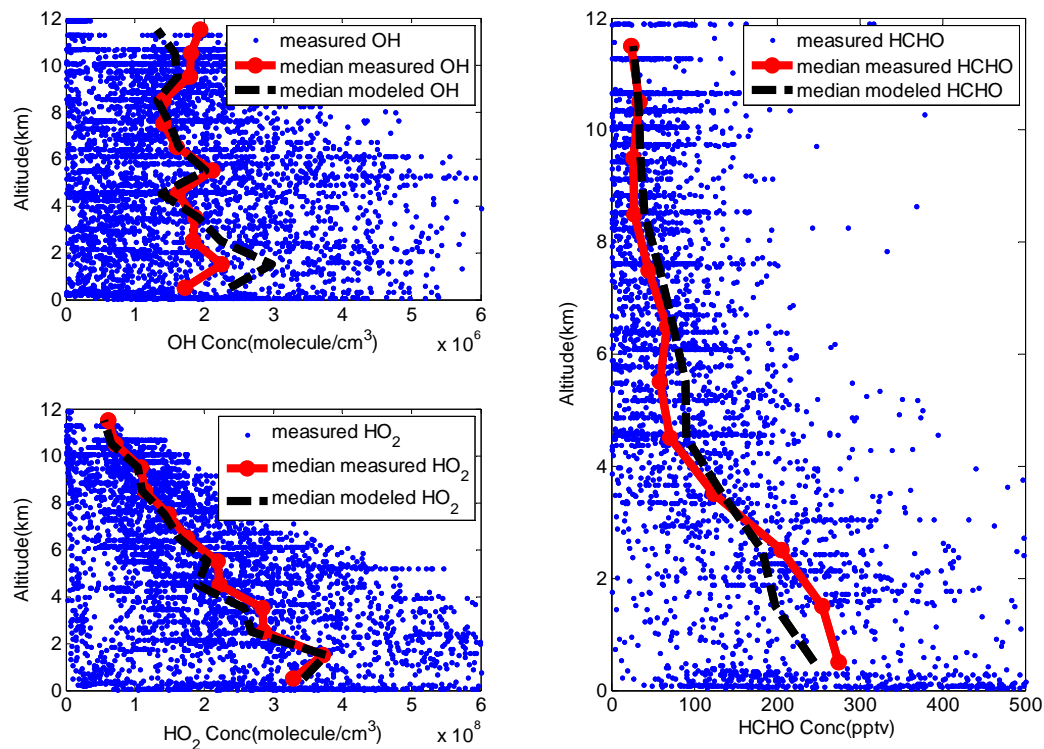


**Fig. 8.** Comparison of median altitude profiles for measured and modeled OH, HO<sub>2</sub> and HCHO during the second phase of INTEX-B. The median measurements are shown as a solid line with circles and the median model calculations are shown as a dashed line. Individual INTEX-B 1-min measurements are also presented (blue dots).

[Title Page](#)[Abstract](#)[Introduction](#)[Conclusions](#)[References](#)[Tables](#)[Figures](#)[◀](#)[▶](#)[◀](#)[▶](#)[Back](#)[Close](#)[Full Screen / Esc](#)[Printer-friendly Version](#)[Interactive Discussion](#)

Airborne  
measurement of OH  
reactivity during  
INTEX-B

J. Mao et al.

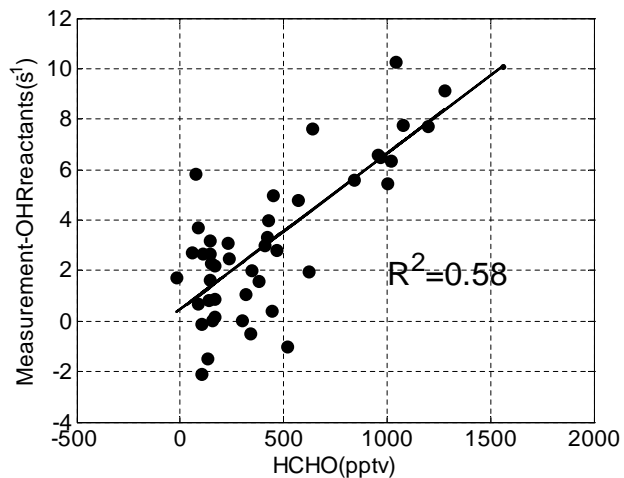


**Fig. 9.** Dependence of difference between OH reactivity measurement and OHRreactants on HCHO below 2 km and when NO is below 100 pptv.

[Title Page](#)[Abstract](#)[Introduction](#)[Conclusions](#)[References](#)[Tables](#)[Figures](#)[⏪](#)[⏩](#)[◀](#)[▶](#)[Back](#)[Close](#)[Full Screen / Esc](#)[Printer-friendly Version](#)[Interactive Discussion](#)